

Tea seed saponin-reduced extract ameliorates palmitic acid-induced insulin resistance in HepG2 cells

SHU-CHI CHO and SHYH-YU SHAW

Department of Chemistry, National Cheng Kung University, Tainan 701, Taiwan, R.O.C.

Received July 19, 2023; Accepted November 29, 2023

DOI: 10.3892/mmr.2023.13149

Abstract. Tea (*Camellia sinensis*) seed cake is a potential resource that contains a wealth of bioactive compounds. However, the high toxicity of tea saponins in tea seed cake restricts its applications. The present study aimed to i) develop a method of extracting bioactive compounds and reducing tea saponins during the process of tea seed cake extraction and ii) investigate the anti-insulin resistance effect of tea seed saponin-reduced extract (TSSRE) in a palmitic acid (PA)-induced insulin resistance HepG2-cell model. The concentration of tea saponins in TSSRE was ~10-fold lower than that in tea seed crude extract (TSCE) after the saponin-reduction process. In addition, TSSRE cytotoxicity was significantly lower than that of TSCE in HepG2 cells. TSSRE treatment improved glucose consumption as well as glucose transporter (GLUT) 2 and GLUT4 expression levels in PA-stimulated HepG2 cells. Moreover, TSSRE enhanced the phosphorylation of the insulin receptor substrate 1/protein kinase B/forkhead box protein O1/glycogen synthase kinase 3 β and inhibited the elevated expression of phosphoenolpyruvate carboxykinase in PA-exposed HepG2 cells. The effect of TSSRE on the mediation of the insulin signaling pathway was attributed to the inhibition of PA-induced mitogen-activated protein kinase activation. The findings of the present study indicated that TSSRE ameliorates hepatic insulin resistance by ameliorating insulin signaling and inhibiting inflammation-related pathways.

Introduction

Diabetes mellitus is a chronic metabolic disorder characterized by high blood sugar levels (hyperglycemia) and a concurrent gradual and irreversible decline in pancreatic insulin secretion over a prolonged period (1,2). Of all types of diabetes mellitus, type 2 diabetes mellitus accounts for ~90% of cases (3). Insulin resistance, also known as impaired insulin sensitivity, is a pathological state of insulin sensitivity where cells do not respond properly to the signal from insulin (4). Insulin-sensitive tissues, such as skeletal muscle, adipose tissue and liver tissue, exhibit diminished glucose uptake into the cytoplasm in patients with insulin resistance (5). Severely, long-term insulin resistance causes hyperglycemia and hyperinsulinemia, eventually leading to type 2 diabetes mellitus (5).

Insulin resistance is mainly linked to an elevated free fatty acid (FFA) content in the blood resulting from a high-calorie diet (4). After binding to an insulin receptor, insulin initiates the downstream signaling pathway to maintain glucose homeostasis in the liver (6). However, excess circulating FFAs in the blood lead to lipid accumulation, causing impaired insulin signaling (7). Several serine kinases, including p38, extracellular signal-regulated kinase (ERK), and c-Jun-N-terminal kinase (JNK), are activated by FFA accumulation and FFA metabolites (8,9). These serine kinases suppress insulin receptor substrate 1 (IRS1) phosphorylation, thereby inhibiting downstream phosphorylation of protein kinase B (Akt) (10-12). In liver tissue, glycogen synthase kinase 3 β (GSK-3 β) and forkhead box protein O1 (FOXO1) are activated by the reduction in Akt activity, leading to decreased glycogen synthesis and elevated gluconeogenesis, which are critical factors in the development of hepatic insulin resistance (13,14). Therefore, targeting the IRS1/Akt/GSK-3 β /FOXO1 signaling pathway is considered a key factor in insulin resistance therapy (15).

Camellia sinensis (*C. sinensis*), known as the tea plant, is an evergreen, medium-sized woody shrub widely distributed across China, Taiwan and Southeast Asia (16). The leaves and leaf buds of *C. sinensis* are used to produce the most commonly consumed non-alcoholic beverage, tea. In addition to its high economic value, *C. sinensis* reportedly provides numerous health benefits for humans, such as anticancer activity, antioxidant activity, cardiovascular benefits and anti-diabetic effects (17). Tea seed, that is, the seed of *C. sinensis*, is typically used to produce tea seed oil, which comprises ~80% unsaturated fatty acids (18). Defatted tea seed, namely, tea

Correspondence to: Dr Shyh-Yu Shaw, Department of Chemistry, National Cheng Kung University, 1 University Road, Tainan 701, Taiwan, R.O.C.

E-mail: syshaw@mail.ncku.edu.tw

Abbreviations: TSSRE, tea seed saponin-reduced extract; TSCE, tea seed crude extract; PA, palmitic acid; GLUT, glucose transporter; IRS1, insulin receptor substrate 1; Akt, protein kinase B; FOXO1, forkhead box protein O1; MAPK, mitogen-activated protein kinase; GSK-3 β , glycogen synthase kinase 3 β

Key words: TSSRE, TSCE, tea saponins, insulin resistance, MAPK

seed cake, is an agricultural byproduct that contains numerous bioactive compounds, rendering it a promising resource. (19). For instance, tea seed cake extract exerts an effect on 5-reductase inhibition (20). Moreover, a kaempferol triglycoside purified from tea seed cake was found to attenuate lipopolysaccharide (LPS)-stimulated inflammation and cognitive impairment in a mouse model (21), and flavonoids separated from tea seed cake also proved to ameliorate tumor necrosis factor alpha (TNF- α)-induced insulin resistance in HepG2 cells (22). However, the high toxicity of tea saponins restricts the application of tea seed cake in livestock feed production or supplementation (23).

Oleiferasaponin B₂, a tea saponin, exhibits strong cytotoxicity with a half maximal inhibitory concentration (IC₅₀) of 6.3 mM (SK-OV-3), 0.8 mM (HCT15), 9.2 mM (SK-MEL-2) and 8.4 mM (A549), while oleiferasaponin B₁ exhibits IC₅₀ values of 11.3 mM (SK-OV-3), 1.6 mM (HCT15), 13.9 mM (SK-MEL-2) and 18.5 mM (A549) (24). Furthermore, a few tea saponins, including floratheasaponins D, E, F and G, have been reported to display potent cytotoxic activity ranging from 6 to 10 μ M in RAW 264.7 cells (25). In addition to their toxicity to cell lines, the toxicity of saponins to cold-blooded animals and insects has also been mentioned in several studies (26). A saponin toxicity assay revealed hemorrhage and erosion of the mucosa in the small intestine as well as necrosis of liver cells and renal tubules in a mouse model (27). Presently, several methods are employed to reduce or remove tea saponins from tea seed cake or tea seed cake extract. For instance, tea saponin levels in tea seed cake are significantly lessened by chemical treatment or biodegradation (28); furthermore, semi-preparative high-performance liquid chromatography (HPLC) can be used to isolate non-catechin flavonoids from saponin-rich tea seed extract (22). However, these saponin-reduction processes can also lead to a reduction in bioactive compounds or the production of lower yields of bioactive compounds. Thus, methods of reducing or eliminating saponins in tea seed cake must be optimized.

Therefore, the present study aimed to i) use chemical treatment to reduce tea saponin levels and separate bioactive molecules from the tea seed crude extract (TSCE) of *C. sinensis* and ii) analyze the anti-insulin resistance effect of the saponin-reduced extract of *C. sinensis* in the HepG2 cell line.

Materials and methods

Preparation of tea seed saponin-reduced extract (TSSRE) from C. Sinensis tea seeds. *C. sinensis* (L.) O. Kuntze is an economic crop in Taiwan; there might be not any policy to regulate the permission of using *C. sinensis* implementing experiment in Taiwan. Specimen of *C. sinensis* identified by Kuoh-Cheng Yan is stored in public at the herbarium of the Research Center for Biodiversity, Academia Sinica, Taipei (HAST). The seeds of *C. sinensis* (L.) O. Kuntze were cultivated in Taitung, Taiwan. They were ground into tea seed powder, which was subsequently stirred in hexane (1:10 w/v) at room temperature for 40 min to simulate tea seed cake. The defatted tea seed powder was subsequently extracted in 95% ethanol (1:10 w/v) for 24 h to obtain TSCE. Thereafter, TSCE was dissolved in 80% ethanol (1:20 w/v). Ethyl acetate

was then mixed with TSCE for precipitation (3:1 v/v). After centrifugation at 3,800 x g for 10 min, the supernatant was evaporated and lyophilized to obtain TSSRE powder.

Determination of the saponin content in TSCE and TSSRE. The tea saponin content in TSSRE was determined as previously reported, with some modifications (29). TSCE, TSSRE and tea saponins (ChemFaces; cat. no. CFN91688) were dissolved in methanol. The samples were mixed with 8% vanillin (Thermo Fisher Scientific, Inc.; cat. no. A11169), followed by 77% sulfuric acid. After mixing, the samples were heated to 65°C for 15 min and subsequently cooled for 10 min. Absorbance values were measured at 505 nm and 510 nm using a microplate reader (SpectraMax Plus 384; Molecular Devices, LLC), and the difference between the absorbance values at these wavelengths reflected tea saponin content.

HPLC analysis of TSSRE. The chromatographic separation of compounds from TSSRE was conducted using an HPLC system (JASCO) and a Hypersil GOLD™ C18 column (250x4.6 mm i.d., 5 μ m; Thermo Fisher Scientific, Inc.). The mobile phase comprised solvents A (0.2% phosphoric acid water) and B (acetonitrile), which were pumped at a flow rate of 1.0 ml/min. 10 μ l sample was injected by an autosampler (JASCO). The gradient elution program was conducted under the following conditions: 0-20 min and 95% A to 40% A. Catechin (MedChemExpress; cat. no. HY-B1890), pyrruside B (ChemFaces; cat. no. CFN96142), narirutin (ChemFaces; cat. no. CFN99543), and naringin (MedChemExpress; cat. no. HY-N0153) were used as the standards.

Determination of the total flavonoid content in TSSRE. The total flavonoid content in TSSRE was estimated using the aluminum chloride colorimetric and 2,4-dinitrophenylhydrazine methods (30,31), and calculated as the sum of the results obtained from these methods.

The aluminum chloride colorimetric method was employed to estimate the levels of flavones and flavonols, which are subclasses of flavonoids. Briefly, 200 μ l of sample was mixed with 40 μ l of 10% aluminum chloride (Thermo Fisher Scientific, Inc.; cat. no. A11892), followed by 600 μ l of 95% ethanol, 20 μ l of 1 M potassium acetate, and 1,120 μ l of distilled water. The mixture was incubated in the dark at room temperature for 30 min. The absorbance values of the samples and standard (quercetin) (MedChemExpress; cat. no. HY-18085) were measured at 415 nm using a microplate reader.

To estimate the levels of flavanones and flavanonols, which are also subclasses of flavonoids, the 2,4-dinitrophenylhydrazine method was employed. Briefly, 200 μ l of sample was mixed with 400 μ l of 1% 2,4-dinitrophenylhydrazine reagent (Sigma-Aldrich; Merck KGaA; cat. no. D199303), followed by 400 μ l of methanol at 50°C for 50 min. After cooling, the mixture was mixed with 1,000 μ l of 1% potassium hydroxide dissolved in 70% methanol and kept at room temperature for 2 min. A total of five times the volume of methanol was mixed with the sample and subsequently centrifuged at 1,000 x g for 10 min at 25°C. After centrifugation, the absorbance values of the supernatant and standard (naringenin) (MedChemExpress; cat. no. HY-W011641) were determined at 495 nm using a microplate reader.

Cell culture. The HepG2 cell line (cat. no. RM60025) was obtained from the Bioresources Collection and Research Center of the Food Industry Research and Development Institute (Hsinchu, Taiwan). HepG2 cells were cultured in high-glucose Dulbecco's Modified Eagle Medium (HyClone; Cytiva; cat. no. SH30243) with 10% fetal bovine serum (HyClone; Cytiva; cat. no. SH30396) containing 100 units/ml penicillin and 0.1 mg/ml streptomycin (BioConcept Ltd.; cat. no. 4-01F00-H) at 37°C with 5% CO₂. The medium was altered every 2 days, and the cells were maintained in culture by passaging them with 0.25% trypsin (HyClone; Cytiva; cat. no. SH30042).

Cell viability assay. HepG2 cells (1x10⁴ cells/well) were cultured in 96-well microtiter plates. After 24-h incubation at 37°C, the HepG2 cells were treated with various concentrations of TSCE and TSSRE for 24 h. Subsequently, 200 µl of 3-(4,5-Dimethylthiazol-2-yl)-2,5-diphenyltetrazolium bromide (MTT) reagent (Sigma-Aldrich; Merck KGaA; cat. no. 475989) was added to each well, and the plates were incubated at 37°C with 5% CO₂ in the dark for 4 h. Thereafter, 150 µl of dimethyl sulfoxide was added to each well, and the plates were subsequently shaken on a shaker at room temperature for 10 min. The absorbance values of the samples were determined at 490 nm using a microplate reader.

Glucose consumption assay. Insulin resistance was induced in a HepG2 cell model using palmitic acid (PA) according to a method previously described, with some modifications (32). Normal glucose (5.5 mM) (HyClone; Cytiva; cat. no. SH30021) was used as the control. Normal glucose group was adopted to simulate the condition of normal and healthy cells (33), which i) evaluated if TSSRE could recover cells to the normal and healthy condition and ii) analyzed how the level of improvement of insulin resistance the drug could affect cells with insulin resistance. HepG2 cells (4x10⁴ cells/well) were cultured in 96-well microtiter plates. After 24-h incubation at 37°C, the cells were washed twice with phosphate-buffered saline (PBS) and subsequently treated with normal-(5.5 mM) or high-concentration (30 mM) glucose plus 0.25 mM PA (Thermo Fisher Scientific, Inc.; cat. no. AC416700050) in the absence or presence of the indicated concentrations of TSSRE for 24 h. Thereafter, 100 nM of insulin (MedChemExpress; cat. no. HY-P73243) was added to each sample, and the plates were incubated at 37°C with 5% CO₂ for 30 min. The cells were washed twice with PBS, and RPMI-1640 (HyClone; Cytiva; cat. no. SH30027) containing 0.2% fatty acid-free bovine serum albumin (BSA, Bio Basic; cat. no. AD0023) was subsequently added to each well. After 24-h incubation at 37°C, the medium was collected for further assay. Each sample (25 µl) was mixed with 500 µl of o-toluidine (Abbkine Scientific Co., Ltd.; cat. no. KTB1300). The mixtures were heated in boiling water for 8 min and subsequently cooled down. The absorbance values of the samples were determined at 630 nm using a microplate reader. RPMI-1640 contains a suitable concentration of glucose (11.1 mM) compared with high glucose DMEM (25 mM) and low glucose DMEM (5 mM) for this assay.

Western blot analysis. HepG2 cells (5x10⁵ cells/well) were cultured in six-well plates. After incubation for 24 h, the HepG2 cells were washed twice with PBS and incubated with

normal-(5.5 mM) or high-concentration (30 mM) glucose plus 0.25 mM PA in the absence or presence of the indicated concentrations of TSSRE. After 24-h treatment, 100 nM of insulin was added to each well for 30 min. The HepG2 cells were washed twice with cold PBS and lysed in radioimmunoprecipitation assay buffer (BIOTOOLS; cat. no. TAAR-ZBZ5) supplemented with protease (BIOTOOLS; cat. no. TAAR-BBI2) and phosphatase (BIOTOOLS; cat. no. TAAR-WBC1) inhibitor cocktails at 0°C. After being scraped off the six-well plates, the cell lysates were collected, transferred to microcentrifuge tubes, and centrifuged (16,500 x g, 20 min, 4°C); thereafter, the supernatants were collected as protein samples. Bicinchoninic acid protein assay reagents (Visual Protein; BC03-500) were utilized to determine the total protein concentration of each sample using a standard BSA curve. The protein samples were diluted to equal amounts of protein and 20 µl/lane was subsequently separated via 8 or 10% sodium dodecyl sulfate-polyacrylamide gel electrophoresis. Thereafter, the gels were transferred to polyvinylidene difluoride (PerkinElmer, Inc.; cat. no. NEF1002001PK) membranes for 2 h. The membranes were blocked for 1 h at room temperature with 5% BSA buffer. After blocking, these membranes were incubated with the following primary antibodies at 4°C overnight: Phosphorylated (p-)p38 (cat. no. 4511; 1:1,000), p38 (cat. no. 8690; 1:1,000), p-ERK (cat. no. 4370; 1:1,000), ERK (cat. no. 4695; 1:1,000), p-JNK (cat. no. 4668; 1:1,000), JNK (cat. no. 9252; 1:1,000), p-Akt (cat. no. 9271; 1:1,000), Akt (cat. no. 9272; 1:1,000), p-IRS1 (cat. no. 3070; 1:1,000), IRS1 (all from Cell Signaling Technology, Inc.; cat. no. 2382; 1:1,000), phosphoenolpyruvate carboxykinase (PEPCK; cat. no. E-AB-11396; 1:1,000), p-GSK-3β (cat. no. E-AB-20886; 1:1,000), GSK-3β (cat. no. E-AB-31629; 1:1,000), glucose transporter (GLUT) 4 (all from Elabscience Biotechnology, Inc.; cat. no. E-AB-30268; 1:1,000), GLUT2 (Proteintech Group, Inc.; cat. no. 20436-1-AP; 1:1,000), p-FOXO1 (cat. no. AF3417; 1:1,000), FOXO1 (both from Affinity Biosciences; cat. no. AF6416; 1:1,000), and β-actin (iReal Biotechnology, Inc.; cat. no. IR2-7; 1:1,000). The membranes were washed thrice with Tris-buffered saline with 0.1% Tween 20 and subsequently incubated with horseradish peroxidase-conjugated secondary antibodies (Abcam; cat. no. ab6721; 1:10,000) at room temperature for 1 h. The immunoblots were visualized using an enhanced chemiluminescence reagent (Visual Protein; cat. no. LF08-500) and captured using a chemiluminescence imaging system. Relative protein levels were quantified using ImageJ software (version 1.8.0; National Institutes of Health), and β-actin was employed as the internal control.

Statistical analysis. Data are presented as the mean ± standard deviation of three independent experiments. GraphPad Prism 9.0 software (Dotmatics) was employed to evaluate statistical differences between groups. P<0.05 was considered to indicate a statistically significant difference based on one-way ANOVA followed by Dunnett's multiple comparisons test.

Results

TSSRE saponin content. The saponin content in TSSRE was measured using the vanillin-sulfuric acid method (Table I). The tea saponin concentrations in TSCE and TSSRE were 5.34±0.46 and 0.54±0.07 mg/g, respectively.

Table I. The saponin contents in TSCE and TSSRE measured by vanillin-sulfuric acid assay.

Extract	Saponin content (mg/g)
TSCE	5.34±0.46
TSSRE	0.54±0.07

TSSRE, tea seed saponin-reduced extract; TSCE, tea seed cake crude extract.

Identification of TSSRE. As revealed in Fig. 1A and B, TSSRE yielded several chromatographic peaks, and the major peaks represented catechin, pyrruside B, narirutin and naringin, identified at the same time points as the standards.

The total flavonoid content in TSSRE. The total flavonoid content in TSSRE was measured using the aluminum chloride colorimetric and 2,4-dinitrophenylhydrazine methods (Table II). In TSSRE, the aluminum chloride assay revealed a flavone and flavonol content of 13.56±1.15 mg/g, while the 2,4-dinitrophenylhydrazine assay revealed a flavanone and flavanonol content of 68.84±7.53 mg/g. Therefore, the total flavonoid content in TSSRE was 82.40±8.68 mg/g.

Cell viability. HepG2 cells were treated with different concentrations of TSCE and TSSRE to evaluate their cell viability. The cell viability assay results are demonstrated in Fig. 2. The cell viability of HepG2 cells significantly declined following 24-h treatment with 32 and 64 µg/ml TSCE (Fig. 2A; 80 and 25%, respectively; P=0.0084 and P<0.0001, respectively) but did not differ significantly at concentrations of 16, 32 and 64 µg/ml from that of the untreated group (Fig. 2B; P=0.9999, P=0.9741 and P=0.999, respectively).

Effect of TSSRE on glucose consumption. Impaired glucose uptake in liver tissues is a characteristic of insulin resistance (5). Therefore, the effect of TSSRE on glucose consumption in PA-triggered insulin-resistant HepG2 cells was investigated (Fig. 3). Glucose consumption in these cells significantly decreased after exposure to 0.25 mM PA compared with that after normal-glucose treatment (3.2-fold). The effect of treatment with 16, 32 and 64 µg/ml TSSRE was not significantly different compared with normal-glucose treatment (P=0.9442, P=0.8796 and P=0.9992, respectively). However, treatment with 32 and 64 µg/ml TSSRE ameliorated glucose consumption in PA-stimulated insulin-resistant HepG2 cells (1.3- and 2.4-fold, respectively; P=0.0064 and P<0.0001, respectively). These results suggested that TSSRE enhanced glucose consumption in PA-stimulated insulin-resistant HepG2 cells. Therefore, treatment with TSSRE in PA-stimulated groups was adopted to implement the further experiments.

Effect of TSSRE on the expression levels of GLUT2 and GLUT4. GLUT2 facilitates glucose transportation across the cell membrane (34). The effect of TSSRE on GLUT2 in PA-stimulated insulin-resistant HepG2 cells was analyzed (Fig. 4A). In the present study, GLUT2 expression in PA-induced

insulin-resistant HepG2 cells was significantly lower than that in the normal-glucose group (2.2-fold). However, 64 µg/ml TSSRE treatment ameliorated GLUT2 expression in these cells (1.8-fold; P<0.0001). GLUT4, an insulin-regulated GLUT, mediates glucose uptake (34). The effect of TSSRE on GLUT4 in PA-stimulated insulin-resistant HepG2 cells was evaluated (Fig. 4B). GLUT4 expression in these cells was significantly lower than that in the normal-glucose group (2.4-fold). However, treatment with 32 and 64 µg/ml TSSRE elevated GLUT4 expression in HepG2 cells with PA-induced insulin resistance (1.2- and 2.4-fold, respectively; P=0.0077 and P<0.0001, respectively). These results suggested that TSSRE ameliorated the expression levels of GLUT2 and GLUT4 in PA-stimulated insulin-resistant HepG2 cells.

Effect of TSSRE on the IRS1/Akt signaling pathway. The IRS1/Akt signaling pathway was investigated to elucidate the mechanism by which TSSRE ameliorates GLUT4 expression in PA-induced insulin-resistant HepG2 cells. The effect of TSSRE on IRS1 in these cells was investigated (Fig. 5A). In the present study, IRS1 phosphorylation was evidently decreased by PA treatment compared with that in the normal-glucose group in HepG2 cells (4.2-fold). However, treatment with 32 and 64 µg/ml TSSRE significantly improved IRS1 phosphorylation (2.2- and 3.3-fold, respectively; P=0.0037 and P<0.0001, respectively). The effect of TSSRE on Akt in PA-induced insulin-resistant HepG2 cells was analyzed (Fig. 5B). Akt phosphorylation in these cells decreased significantly in the present study (3.6-fold). TSSRE treatment at 32 and 64 mg/ml significantly ameliorated Akt phosphorylation (1.8- and 2.5-fold, respectively; P=0.0070, and P=0.0002, respectively). These results demonstrated that TSSRE enhanced the IRS1/Akt signaling pathway in PA-stimulated insulin-resistant HepG2 cells.

Effect of TSSRE on PEPCK and FOXO1. PEPCK is an enzyme involved in gluconeogenesis, a process in which glucose is synthesized from non-hexose precursors (35). The effect of TSSRE on PEPCK in PA-stimulated insulin-resistant HepG2 cells was evaluated (Fig. 6A). PEPCK expression increased significantly in these cells compared with that in the normal-glucose group (2.1-fold). However, treatment with 32 and 64 mg/ml TSSRE reduced PEPCK expression in PA-triggered insulin-resistant HepG2 cells (1.3- and 2.1-fold, respectively; P=0.0034 and P<0.0001, respectively). FOXO1, a transcription factor, regulates gluconeogenesis (14). The effect of TSSRE on FOXO1 in PA-induced insulin-resistant HepG2 cells was investigated (Fig. 6B). FOXO1 phosphorylation declined significantly after 24-h PA treatment (2.4-fold). TSSRE treatment at 32 and 64 mg/ml significantly improved FOXO1 phosphorylation in PA-triggered insulin-resistant HepG2 cells (1.8- and 2.6-fold, respectively; P=0.0054 and P<0.0001, respectively).

Effect of TSSRE on GSK-3β phosphorylation. GSK-3β has been known to play a critical role in inhibiting the activity of glycogen synthase (13). The effect of TSSRE on GSK-3β in PA-stimulated insulin-resistant HepG2 cells was analyzed (Fig. 7). In the present study, GSK-3β phosphorylation decreased significantly in these cells compared with that in the

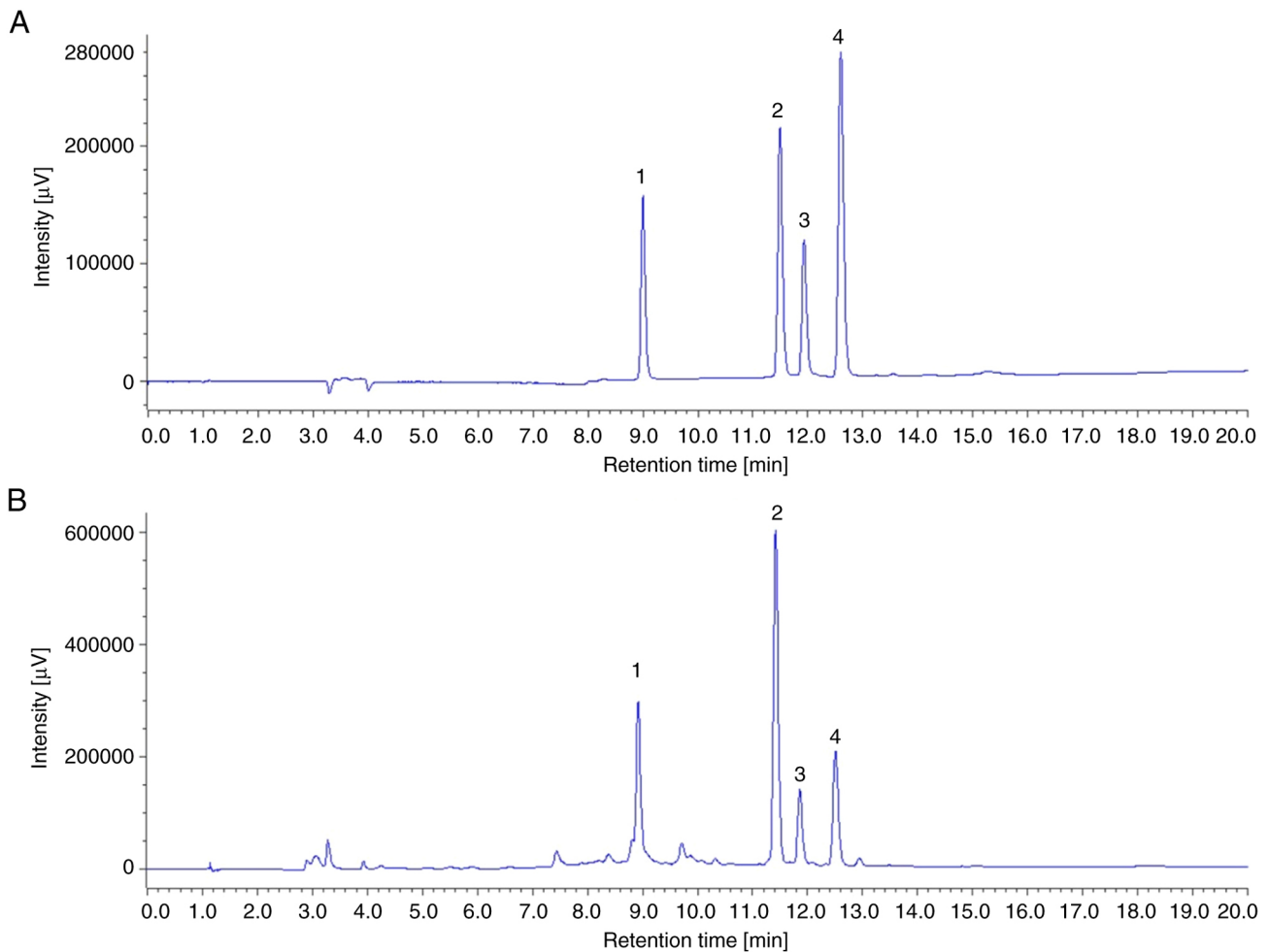


Figure 1. HPLC analysis of (A) standards and (B) tea seed saponin-reduced extract. Peak identification: (1) Catechin, (2) pyrruside B, (3) narirutin and (4) naringin.

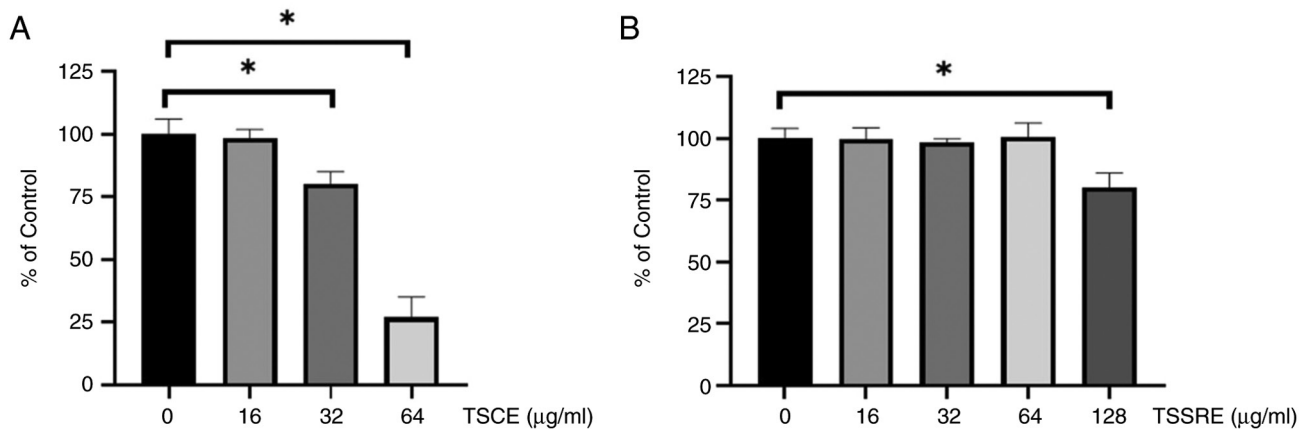


Figure 2. Cell viability of TSCE and TSSRE in HepG2 cells. (A) HepG2 cells were treated with various concentrations of TSCE for 24 h. (B) HepG2 cells were treated with various concentrations of TSSRE for 24 h. HepG2 cells were treated with normal-(5.5 mM) or high-concentration (30 mM) glucose with palmitic acid (0.25 mM) in the absence or presence of TSSRE for 24 h. *P<0.05. TSCE, tea seed cake crude extract; TSSRE, tea seed saponin-reduced extract.

normal-glucose group (2.7-fold). TSSRE treatment at 16, 32, and 64 mg/ml notably ameliorated GSK-3β phosphorylation in PA-induced insulin-resistant HepG2 cells (2.1-, 2.5- and 2.7-fold, respectively; P=0.0001, P<0.0001 and P<0.0001, respectively).

Effect of TSSRE on the phosphorylation of JNK, p38 and ERK. JNK, p38 and ERK suppress IRS1 phosphorylation (10-12). The effect of TSSRE on the LPS-stimulated phosphorylation of mitogen-activated protein kinases (MAPKs), that is, p38, ERK and JNK, was explored using western blot analysis (Fig. 8).

Table II. The flavonoid contents in TSSRE measured by aluminum chloride and 2,4-dinitrophenylhydrazine colorimetric assays.

Extract	Flavonoid content (mg/g)		
	AlCl ₃	2,4-D	Total
TSSRE	13.56±1.15	68.84±7.53	82.40±8.68

TSSRE, tea seed saponin-reduced extract; 2,4-D, 2,4-dinitrophenylhydrazine.

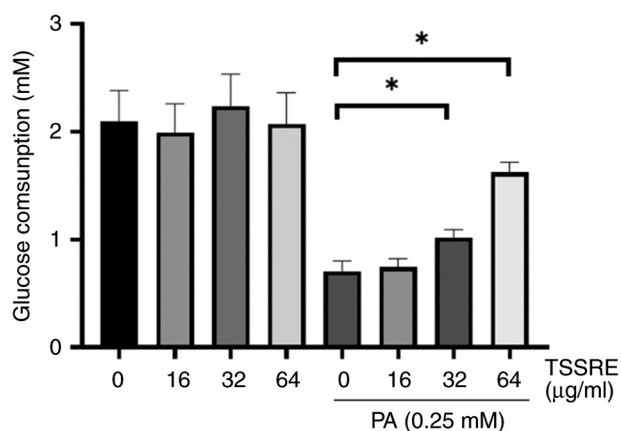


Figure 3. Effects of TSSRE on glucose consumption in HepG2 cells. HepG2 cells were treated with normal-(5.5 mM) or high-concentration (30 mM) glucose with PA (0.25 mM) in the absence or presence of TSSRE for 24 h and subsequently treated with insulin (100 nM) for 30 min. *P<0.05. TSSRE, tea seed saponin-reduced extract; PA, palmitic acid.

The results demonstrated that the phosphorylation of p38, ERK and JNK was significantly induced by 24-h stimulation with 0.25 mM PA compared with that in the normal-glucose group in HepG2 cells (11.7-, 3.1- and 3.7-fold, respectively). PA-stimulated p38 phosphorylation was significantly attenuated by TSSRE at concentrations of 32 and 64 µg/ml (1.8- and 3.3-fold, respectively; P=0.0004 and P<0.0001, respectively). Furthermore, TSSRE treatment at 32 and 64 mg/ml also suppressed PA-induced ERK phosphorylation (1.7- and 2.1-fold, respectively; P=0.0003 and P=0.0012, respectively). JNK phosphorylation was also significantly inhibited by TSSRE treatment at 32 and 64 mg/ml in PA-stimulated insulin-resistant HepG2 cells (1.8- and 1.9-fold, respectively; P<0.0001 and P<0.0001, respectively).

Discussion

In the present study, the administration of TSSRE extracted from tea seed cake effectively reversed PA-induced insulin resistance in HepG2 cells. Tea seed cake is an agricultural residue that remains after tea seed oil extraction. Hence, the efficient utilization of this resource and waste reduction are critical issues in agriculture. Tea seed cake, which comprises 10-16% tea saponins, possesses hemolytic and cytotoxic properties (36,37), and these properties potentially cause

toxicity in cold-blooded animals and mice (38,39). In the present study, a simple, low-cost method was developed to obtain saponin-reduced extract from tea seed cake. After the saponin-reduction process, the tea saponin concentration in TSSRE significantly decreased compared with that in TSCE. The vanillin-sulfuric acid assay demonstrated that the tea saponin concentration in TSSRE was ~10-fold lower than that in TSCE, and this result indicated that this saponin-reduction process could markedly decrease the concentration of tea saponins in TSCE. The MTT assay revealed that only 25% of HepG2 cells survived after 24 h treatment with 64 µg/ml TSCE in the cytotoxicity analysis. However, no significant cytotoxicity was observed in HepG2 cells after treatment with 64 µg/ml TSSRE, suggesting that this saponin-reduction process not only decreased the concentration of tea saponins but also ameliorated their cytotoxic effect in HepG2 cells. HPLC analysis demonstrated that the primary peaks in TSCE represented catechin, pyrsoside B, narirutin and naringin, which are flavonoids, natural substances found in the kingdom of plants (40). The total flavonoid content in TSSRE was determined to be 82.40±8.68 mg/g, and flavanones and flavanonols were the predominant flavonoids (~80%). Among these flavonoids, naringin and catechin have proven effective in improving insulin resistance (41,42). Hence, the anti-insulin resistance effect of TSSRE may be attributed to the presence of these two flavonoids. A previous study also indicated that flavonoids purified from tea seed cake alleviate TNF-α-induced insulin resistance in HepG2 cells (22). Furthermore, numerous flavonoids exerting anti-diabetic and anti-insulin resistance effects have also been reported (43,44).

Dietary habits constitute an important factor contributing to the risk of insulin resistance (45). PA, a 16-carbon-chain fatty acid is the most common saturated fatty acid in the human diet (46). Excessive FFA consumption has proven to be largely associated with the development of metabolic syndrome, such as insulin resistance and type 2 diabetes mellitus (47). In the present study, PA was employed to induce insulin resistance in HepG2 cells. After 24 h of PA exposure, glucose consumption in HepG2 cells was markedly decreased compared with that in the untreated group. Nevertheless, 32- and 64-µg/ml TSSRE treatments significantly reversed the PA-induced impaired glucose consumption. GLUTs constitute a class of membrane proteins that facilitate glucose transportation across the cell membrane (34). Among them, GLUT2 is predominantly found in the β cells of the pancreas, kidney and liver (48). GLUT4, an insulin-dependent GLUT, responds to insulin-stimulated cell signaling to reduce blood glucose levels (34). In the present study, the expression levels of GLUT2 and GLUT4 were decreased by PA treatment compared with those in the normal-glucose group. However, TSSRE treatment ameliorated the PA-induced expression levels of GLUT2 and GLUT4. The present data indicated that TSSRE enhances glucose consumption in PA-stimulated insulin-resistant HepG2 cells by increasing GLUT2 and GLUT4 expression.

The insulin signaling pathway plays an important role in regulating insulin signaling transduction and maintaining glucose homeostasis (6). Upon binding to insulin, the insulin receptor undergoes conformational changes, thereby activating kinase activity (49). Thereafter, downstream IRS1 is recruited

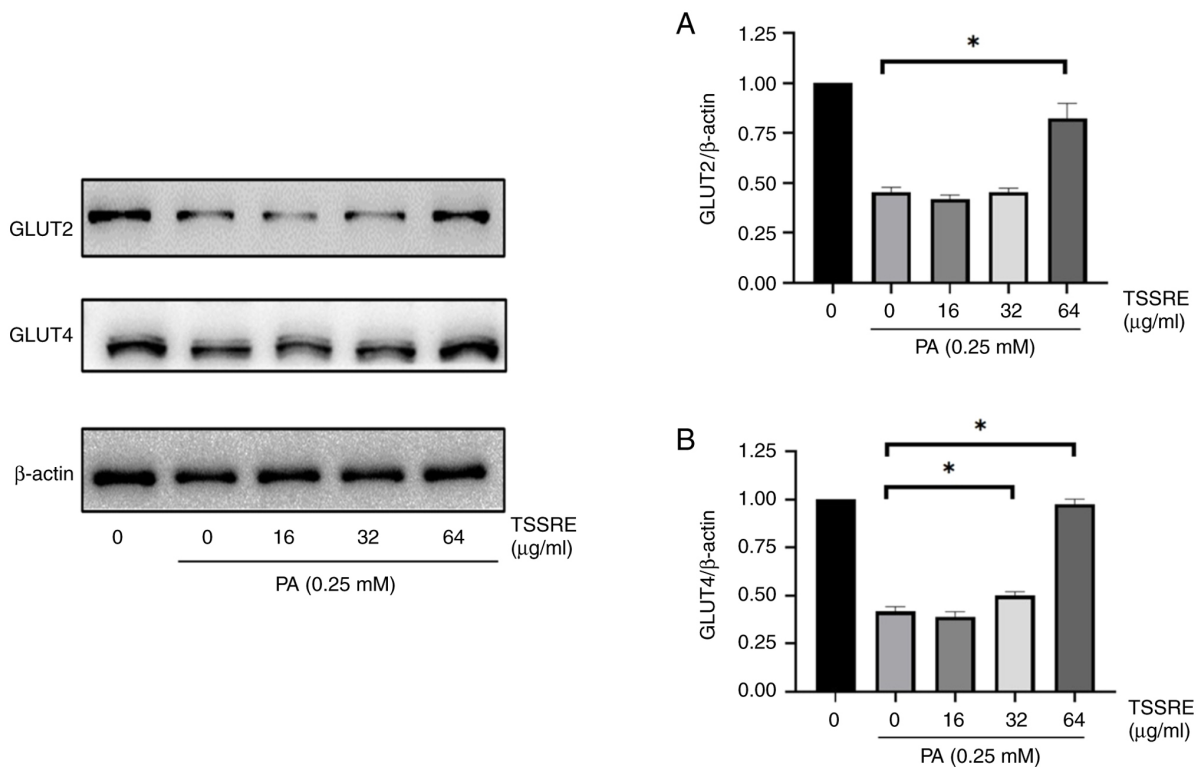


Figure 4. Effects of TSSRE on the expression levels of (A) GLUT2 and (B) GLUT4 in HepG2 cells. HepG2 cells were treated with normal-(5.5 mM) or high-concentration (30 mM) glucose plus 0.25 mM PA in the absence or presence of TSSRE for 24 h and subsequently treated with insulin (100 nM) for 30 min. *P<0.05. TSSRE, tea seed saponin-reduced extract; GLUT, glucose transporter.

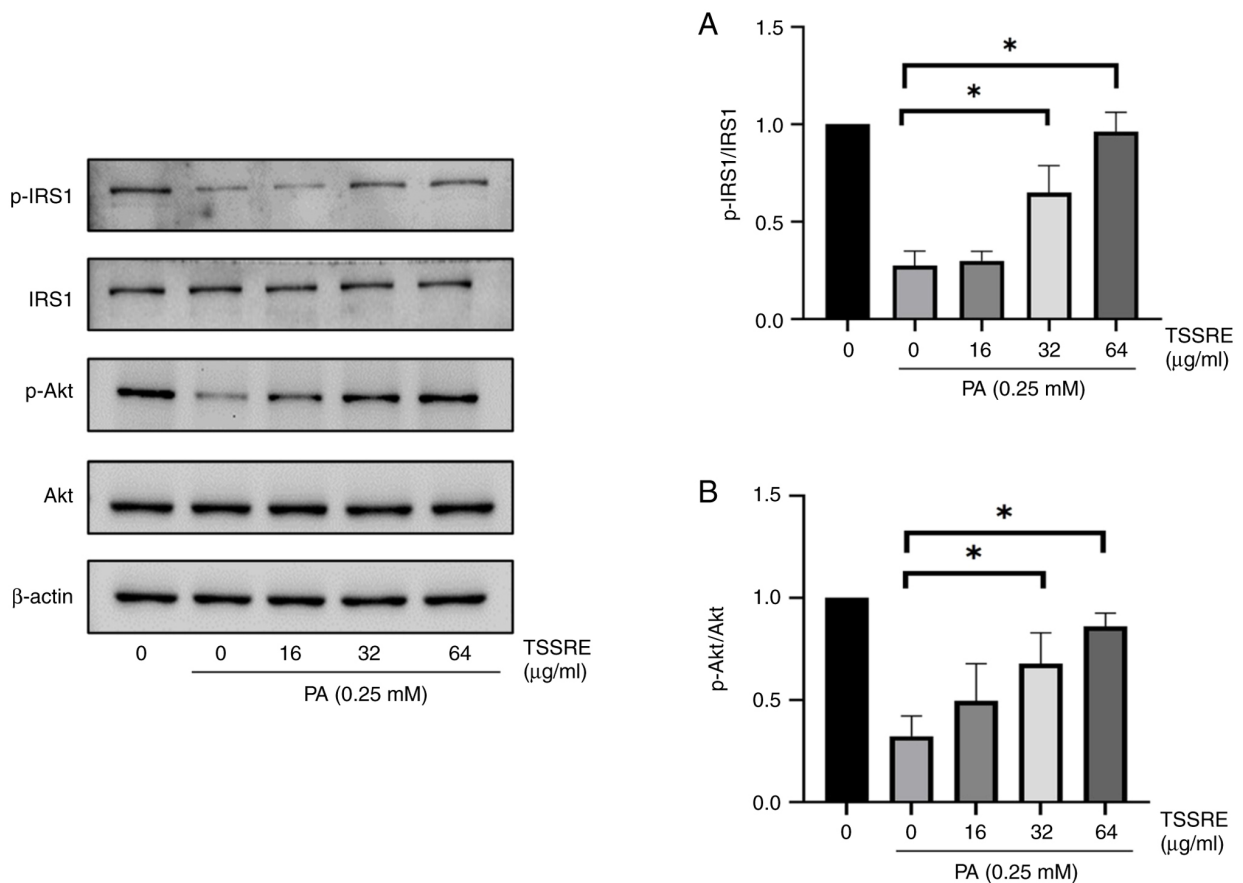


Figure 5. Effects of TSSRE on phosphorylation of (A) IRS1 and (B) Akt in HepG2 cells. HepG2 cells were treated with normal-(5.5 mM) or high-concentration (30 mM) glucose plus 0.25 mM PA in the absence or presence of TSSRE for 24 h and subsequently treated with insulin (100 nM) for 30 min. *P<0.05. TSSRE, tea seed saponin-reduced extract; IRS1, insulin receptor substrate 1; PA, palmitic acid; p-, phosphorylated.

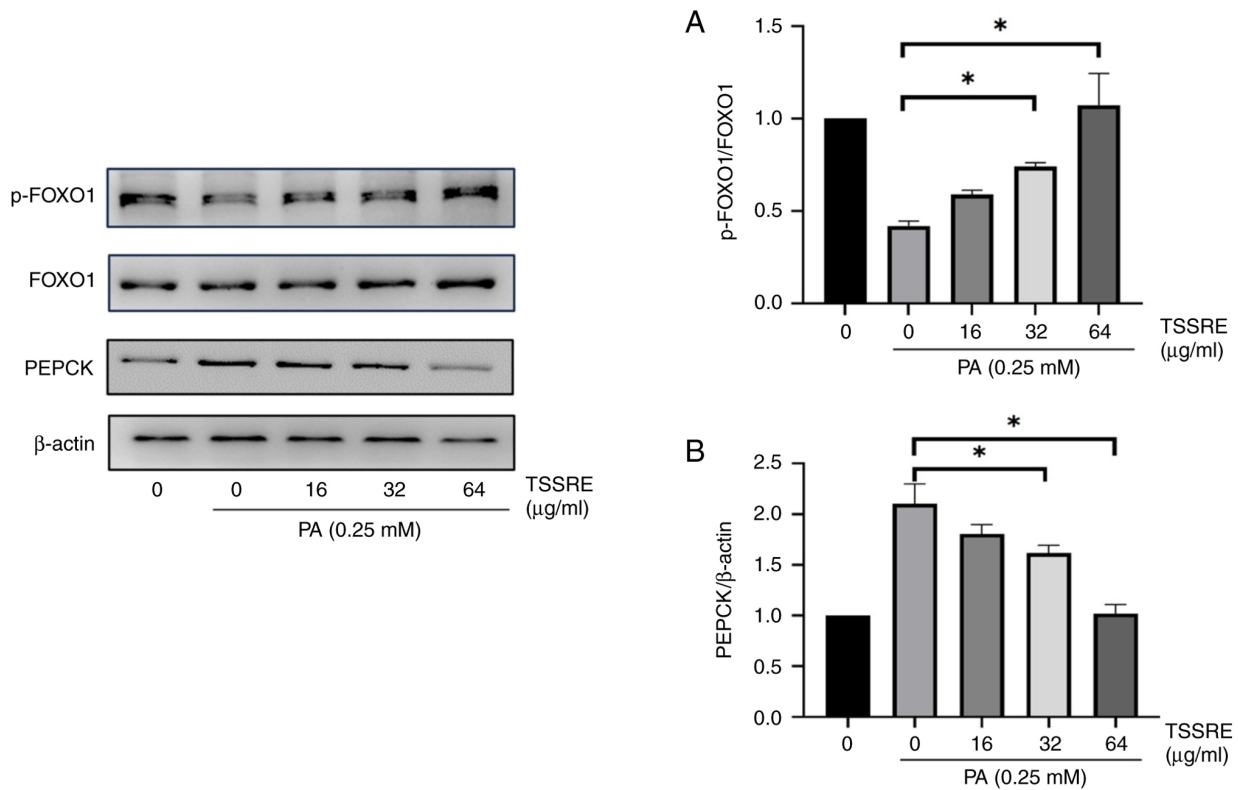


Figure 6. Effects of TSSRE on phosphorylation of (A) FOXO1 and (B) PEPCK in HepG2 cells. HepG2 cells were treated with normal-(5.5 mM) or high-concentration (30 mM) glucose plus 0.25 mM PA in the absence or presence of TSSRE for 24 h and subsequently treated with insulin (100 nM) for 30 min. * $P < 0.05$. TSSRE, tea seed saponin-reduced extract; FOXO1, forkhead box protein O1; PEPCK, phosphoenolpyruvate carboxykinase; PA, palmitic acid; p-, phosphorylated.

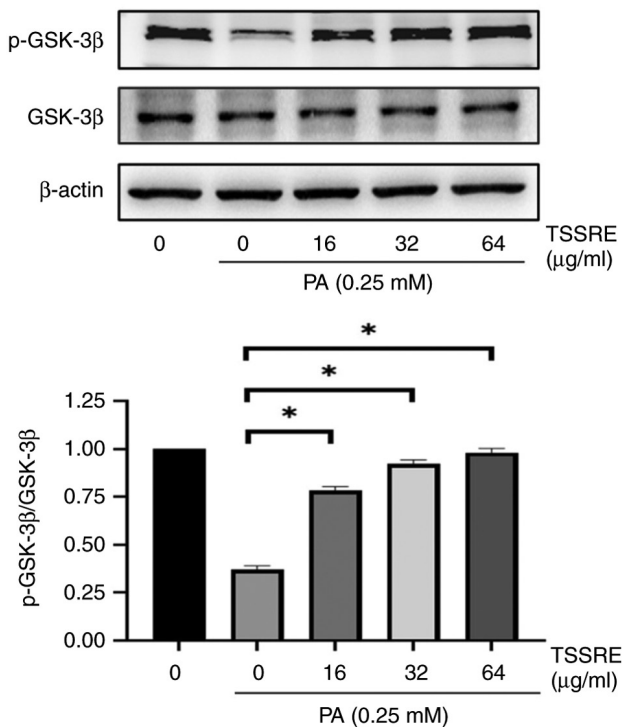


Figure 7. Effects of TSSRE on GSK-3 β phosphorylation in HepG2 cells. HepG2 cells were treated with normal-(5.5 mM) or high-concentration (30 mM) glucose plus 0.25 mM PA in the absence or presence of TSSRE for 24 h and subsequently treated with insulin (100 nM) for 30 min. * $P < 0.05$. TSSRE, tea seed saponin-reduced extract; GSK-3 β , glycogen synthase kinase 3 β ; PA, palmitic acid; p-, phosphorylated.

and phosphorylated (50). IRS1 phosphorylation subsequently stimulates Akt to perform further regulation. The activated IRS1/Akt signaling pathway has proven to increase GLUT4 expression (51). In the present study, p-Akt and p-IRS1 levels were reduced in PA-treated HepG2 cells. However, TSSRE significantly improved PA-induced Akt and IRS1 phosphorylation. These results suggested that TSSRE ameliorated GLUT4 expression by elevating IRS1 and Akt phosphorylation. Since Akt does not regulate GLUT2 expression in the liver (52), the elevated GLUT2 expression in PA-stimulated insulin-resistant HepG2 cells was not regulated through Akt pathway.

In addition to increasing GLUT4 expression, Akt also regulates several factors of glucose metabolism in hepatocytes, such as gluconeogenesis and glycogen synthesis (53). Activated Akt phosphorylates transcription factor FOXO1 to promote FOXO1 efflux from the nucleus into the cytosol, preventing FOXO1 from promoting the transcription of genes involved in gluconeogenesis, such as the gene encoding PEPCK, a key enzyme in gluconeogenesis (14). In insulin resistance, increased hepatic gluconeogenesis leads to excessive glucose production, contributing to elevated blood glucose levels (54). FOXO1 phosphorylation was suppressed in the insulin-resistance group, and increased PEPCK expression was also observed after PA treatment in HepG2 cells. However, TSSRE treatment significantly ameliorated FOXO1 phosphorylation and inhibited PEPCK expression. Therefore, these findings demonstrated the inhibitory effect of TSSRE on gluconeogenesis in HepG2 cells by mediating Akt/FOXO1 signaling.

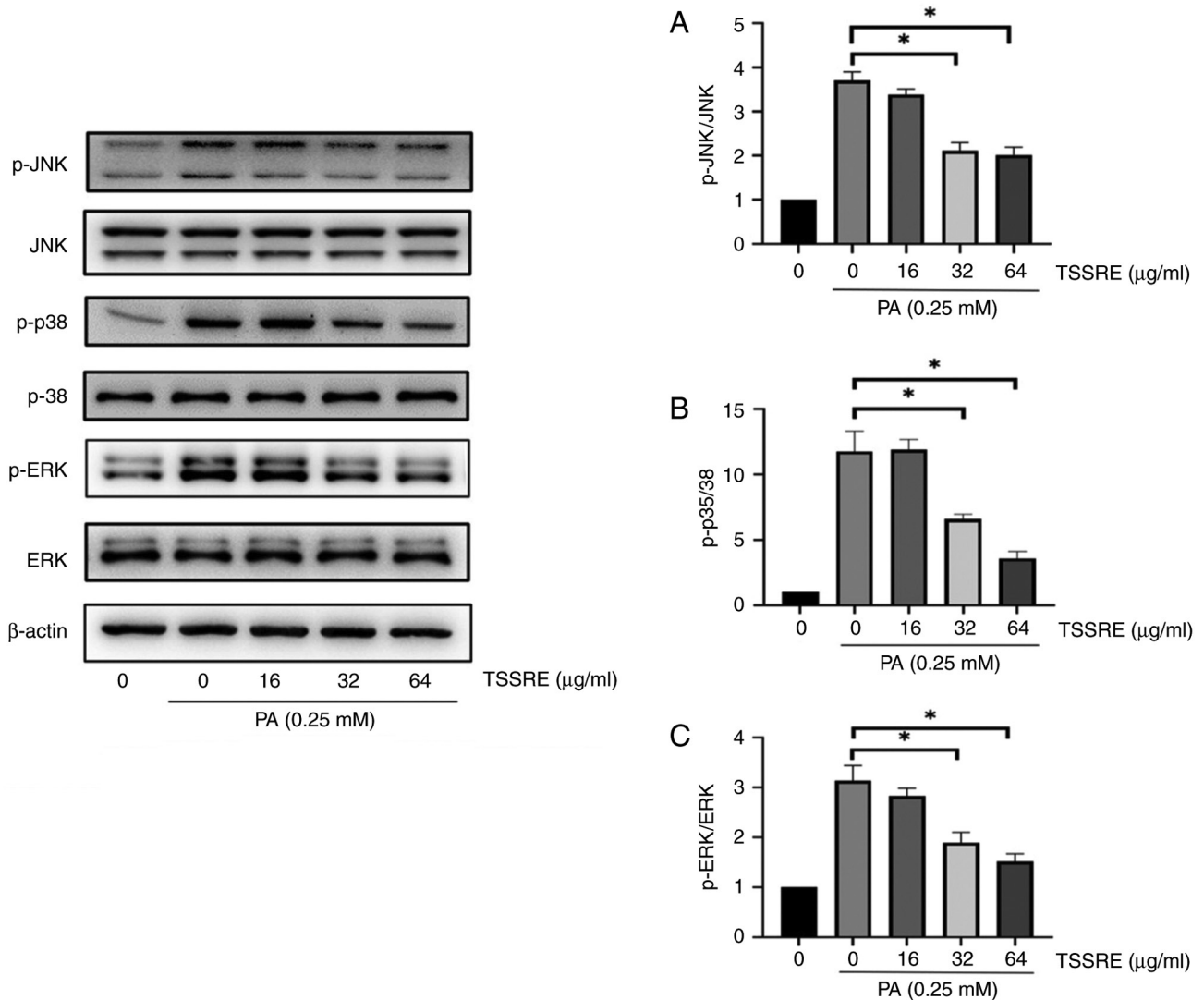


Figure 8. Effects of TSSRE on phosphorylation of (A) JNK, (B) p38 and (C) ERK in HepG2 cells. HepG2 cells were treated with normal-(5.5 mM) or high-concentration (30 mM) glucose plus 0.25 mM PA in the absence or presence of TSSRE for 24 h and subsequently treated with insulin (100 nM) for 30 min. *P<0.05. TSSRE, tea seed saponin-reduced extract; PA, palmitic acid; p-, phosphorylated.

Glycogen, found in muscle and liver tissues, is an extensively branched polysaccharide comprising glucose (55). The liver catabolizes glycogen into glucose, which is subsequently conveyed to the blood and tissues to maintain appropriate blood sugar levels and provide fuel, respectively (55). In insulin resistance, reduced insulin signaling leads to decreased liver glycogen levels (56). Activated Akt serves an essential role in inhibiting GSK-3 β activation by phosphorylating GSK-3 β (13). When Akt is inhibited, GSK-3 β activation decreases the activity of glycogen synthase, a key enzyme involved in glycogen synthesis (13). In the present study, PA was found to inhibit GSK-3 β phosphorylation. Nonetheless, GSK-3 β phosphorylation was significantly elevated by TSSRE treatment in PA-stimulated insulin-resistant HepG2 cells, suggesting that TSSRE inhibits GSK-3 β activation by mediating Akt/GSK-3 β signaling.

The MAPK pathway, a cell signaling pathway, is responsible for transducing various extracellular stimuli to the nucleus, leading to gene regulation (57). It is activated by FFA accumulation, which interferes with IRS1 phosphorylation, thereby inhibiting insulin signal transduction (8). This interference

leads to the disruption of downstream signaling and gene expression, including decreased GLUT4 expression, elevated gluconeogenesis and GSK-3 β activation, which are key factors of insulin resistance (13,14). Hence, further investigation is required to determine whether the amelioration of IRS1 phosphorylation by TSSRE is associated with MAPK inhibition. In the present study, the phosphorylation of p38, ERK and JNK was markedly induced by 24-h PA treatment. TSSRE was found to significantly inhibit the PA-induced phosphorylation of p38, ERK and JNK in HepG2 cells, indicating that TSSRE improves hepatic insulin resistance by suppressing the MAPK pathway (the upstream pathway of IRS1).

Nevertheless, it is important to acknowledge potential limitations in the present study. Given that skeletal muscle plays a pivotal role in utilizing more than 75% of glucose in response to insulin (58), it may be prudent to consider utilizing a skeletal muscle cell line for investigating the anti-insulin resistance effects of TSSRE. Therefore, in the forthcoming research, the authors intend to employ the C2C12 cell line to assess whether TSSRE can ameliorate insulin resistance in skeletal muscle cells.

In conclusion, the current study developed a simple, low-cost method of obtaining saponin-reduced extract from tea seed cake, and treatment with the extract (TSSRE) exhibited significant improvements in glucose homeostasis in PA-stimulated insulin-resistant HepG2 cells. The findings of the present study conclusively demonstrated that TSSRE regulates hepatic insulin resistance by ameliorating the IRS-1/Akt/GSK-3 β /FOXO1 pathway and inhibiting the MAPK pathway. Overall, the beneficial effect of TSSRE in alleviating hepatic insulin resistance was indicated.

Acknowledgements

Not applicable.

Funding

The present study was supported by Higher Education Sprout Project, Ministry of Education to the Headquarters of University Advancement at National Cheng Kung University under Interdisciplinary Research Center on Material and Medicinal Chemistry (D112-G2202).

Availability of data and materials

The datasets used and/or analyzed during the current study are available from the corresponding author on reasonable request.

Authors' contributions

SCC and SYS designed the study. SCC performed the experiments and wrote the manuscript. SYS provided the supervision of the study and was involved in editing and revising of the manuscript. SCC and SYS confirm the authenticity of all the raw data. Both authors read and approved the final version of the manuscript.

Ethics approval and consent to participate

Not applicable.

Patient consent for publication

Not applicable.

Competing interests

The authors declare that they have no competing interests.

References

- Barquilla García A: Brief update on diabetes for general practitioners. *Rev Esp Sanid Penit* 19: 57-65, 2017.
- Ashcroft FM and Rorsman P: Diabetes mellitus and the β cell: The last ten years. *Cell* 148: 1160-1171, 2012.
- Chatterjee S, Khunti K and Davies MJ: Type 2 diabetes. *Lancet* 389: 2239-2251, 2017.
- Xin Y, Wang Y, Chi J, Zhu X, Zhao H, Zhao S and Wang Y: Elevated free fatty acid level is associated with insulin-resistant state in nondiabetic Chinese people. *Diabetes Metab Syndr* 12: 139-147, 2019.
- Honka MJ, Latva-Rasku A, Bucci M, Virtanen KA, Hannukainen JC, Kalliokoski KK and Nuutila P: Insulin-stimulated glucose uptake in skeletal muscle, adipose tissue and liver: A positron emission tomography study. *Eur J Endocrinol* 178: 523-531, 2018.
- Aldhoon-Hainerová I, Zamrazilová H, Dušátková L, Sedláčková B, Hlavatý P, Hill M, Hampl R, Kunešová M and Hainer V: Glucose homeostasis and insulin resistance: Prevalence, gender differences and predictors in adolescents. *Diabetol Metab Syndr* 6: 100, 2014.
- Boden G: 45Obesity, insulin resistance and free fatty acids. *Curr Opin Endocrinol Diabetes Obes* 18: 139-143, 2011.
- Šrámek J, Němcová-Fürstová V and Kovář J: Kinase signaling in apoptosis induced by saturated fatty acids in pancreatic β -cells. *Int J Mol Sci* 17: 1400, 2016.
- Lawan A and Bennett AM: Mitogen-activated protein kinase regulation in hepatic metabolism. *Trends Endocrinol Metab* 28: 868-878, 2017.
- Shin J, Fukuhara A, Onodera T, Kita S, Yokoyama C, Otsuki M and Shimomura I: SDF-1 is an autocrine insulin-desensitizing factor in adipocytes. *Diabetes* 67: 1068-1078, 2018.
- Bengal E, Aviram S and Hayek T: p38 MAPK in glucose metabolism of skeletal muscle: Beneficial or harmful? *Int J Mol Sci* 21: 6480, 2020.
- Feng J, Lu S, Ou B, Liu Q, Dai J, Ji C, Zhou H, Huang H and Ma Y: The role of JNk signaling pathway in obesity-driven insulin resistance. *Diabetes Metab Syndr Obes* 13: 1399-1406, 2020.
- Cross DA, Alessi DR, Cohen P, Andjelkovich M and Hemmings BA: Inhibition of glycogen synthase kinase-3 by insulin mediated by protein kinase B. *Nature* 378: 785-789, 1995.
- Taniguchi CM, Emanuelli B and Kahn CR: Critical nodes in signalling pathways: Insights into insulin action. *Nat Rev Mol Cell Biol* 7: 85-96, 2006.
- Guo S: Molecular basis of insulin resistance: The role of IRS and Foxo1 in the control of diabetes mellitus and its complications. *Drug Discov Today Dis Mech* 10: e27-e33, 2013.
- Yüko K: The spread of tea from Taiwan and the Chinese distribution network in colonial java. *Mem Res Dep Toyo Bunko* 77: 39-64, 2019.
- Aboulwafa MM, Youssef FS, Gad HA, Altyar AE, Al-Azizi MM and Ashour ML: A comprehensive insight on the health benefits and phytoconstituents of *Camellia sinensis* and recent approaches for its quality control. *Antioxidants (Basel)* 8: 455, 2019.
- Zeng W and Endo Y: Lipid characteristics of camellia seed oil. *J Oleo Sci* 68: 649-658, 2019.
- Shen J, Zhang Z, Tian B and Hua Y: Lipophilic phenols partially explain differences in the antioxidant activity of subfractions from methanol extract of camellia oil. *Eur Food Res Technol* 235: 1071-1082, 2012.
- Park JS, Yeom MH, Park WS, Joo KM, Rho HS, Kim DH and Chang IS: Enzymatic hydrolysis of green tea seed extract and its activity on 5 α -reductase inhibition. *Biosci Biotechnol Biochem* 70: 387-394, 2006.
- Yeh TM, Chang CD, Liu SS, Chang CI and Shih WL: Tea seed kaempferol triglycoside attenuates LPS-induced systemic inflammation and ameliorates cognitive impairments in a mouse model. *Molecules* 27: 2055, 2022.
- Chen FC, Shen KP, Ke LY, Lin HL, Wu CC and Shaw SY: Flavonoids from *Camellia sinensis* (L.) O. Kuntze seed ameliorates TNF- α induced insulin resistance in HepG2 cells. *Saudi Pharm J* 27: 507-516, 2019.
- Fu G, Chen K, Wang J, Wang M, Li R, Wu X, Wu C, Zhang P, Liu C and Wan Y: Screening of tea saponin-degrading strain to degrade the residual tea saponin in tea seed cake. *Prep Biochem Biotechnol* 50: 697-707, 2020.
- Chaicharoenpong C: Tea (*Camellia oleifera*) seeds: Use of tea seeds in human health. In: *Nuts and Seeds in Health and Disease Prevention*. Elsevier, pp299-313, 2020.
- Ohta T, Nakamura S, Matsumoto T, Nakashima S, Ogawa K, Matsumoto T, Fukaya M, Yoshikawa M and Matsuda H: Chemical structure of an acylated oleanane-type triterpene oligoglycoside and anti-inflammatory constituents from the flower buds of *Camellia sinensis*. *Nat Prod Commun* 12: 1193-1196, 2017.
- Fan L, He Y, Xu Y, Li P, Zhang J and Zhao J: Triterpenoid saponins in tea (*Camellia sinensis*) plants: Biosynthetic gene expression, content variations, chemical identification and cytotoxicity. *Int J Food Sci Nutr* 72: 308-323, 2021.
- Diwan F, Abdel Hassan I and Mohammed S: Effect of saponin on mortality and histopathological changes in mice. *East Mediterr Health J* 6: 345-351, 2000.

28. Yu Z, Hong H, Xing N, Xi H and Jiang H: Comparison of bio-fermentation and chemical method in the improvement of the quality of oil-tea *Camellia* seed meal. *China Oils Fats* 35: 40-43, 2010.
29. Lai LR, Hsieh SC, Huang HY and Chou CC: Effect of lactic fermentation on the total phenolic, saponin and phytic acid contents as well as anti-colon cancer cell proliferation activity of soymilk. *J Biosci Bioeng* 115: 552-556, 2013.
30. Nagy M and Grancai D: Colorimetric determination of flavanones in propolis. *Pharmazie* 51: 100-101, 1996.
31. Woisky RG and Salatino A: Analysis of propolis: Some parameters and procedures for chemical quality control. *J Apic Res* 37: 99-105, 1998.
32. Zhang Y, Yan LS, Ding Y, Cheng BCY, Luo G, Kong J, Liu TH and Zhang SF: Edgeworthia gardneri (Wall.) Meisn. water extract ameliorates palmitate induced insulin resistance by regulating IRS1/GSK3 β /FoxO1 signaling pathway in human HepG2 hepatocytes. *Front Pharmacol* 10: 1666, 2020.
33. Alnahdi A, John A and Raza H: Augmentation of glucotoxicity, oxidative stress, apoptosis and mitochondrial dysfunction in HepG2 cells by palmitic acid. *Nutrients* 11: 1979, 2019.
34. Cholkar K, Ray A, Agrahari V, Pal D and Mitra AK: Transporters and receptors in the anterior segment of the eye. In: *Ocular Transporters and Receptors*. Elsevier, pp115-168, 2013.
35. Croniger CM, Olswang Y, Reshef L, Kalhan SC, Tilghman SM and Hanson RW: Mini-series: Modern metabolic concepts phosphoenolpyruvate carboxykinase revisited. *Biochem Mol Biol Educ* 30: 14-20, 2002.
36. Chen Y, Gao Y, Han Z and Yin J: Analysis of the saponin contents and composition in tea seeds of different germplasms. *J Tea Sci* 42: 705-716, 2022.
37. Soltani M, Parivar K, Baharara J, Kerachian MA and Asili J: Hemolytic and cytotoxic properties of saponin purified from *Holothuria leucospilota* sea cucumber. *Rep Biochem Mol Biol* 3: 43-50, 2014.
38. Dong Z, Sun T, Liang L and Wang L: Effect of tea saponin on ephyrae and polyps of the moon jellyfish *Aurelia* sp.1. *PLoS One* 12: e0182787, 2017.
39. Ahmed H, Mariod A and Hammada T: The chronic toxicity studies of camellia seed oil containing tea saponins on mice blood and organs. *Int J Life Sci Biotechnol* 4: 178-191, 2021.
40. Waheed Janabi AH, Kamboh AA, Saeed M, Xiaoyu L, BiBi J, Majeed F, Naveed M, Mughal MJ, Korejo NA, Kamboh R, *et al*: Flavonoid-rich foods (FRF): A promising nutraceutical approach against lifespan-shortening diseases. *Iran J Basic Med Sci* 23: 140-153, 2020.
41. Termkwancharoen C, Malakul W, Phetrungnapha A and Tunsophon S: Naringin ameliorates skeletal muscle atrophy and improves insulin resistance in high-fat-diet-induced insulin resistance in obese rats. *Nutrients* 14: 4120, 2022.
42. Wen L, Wu D, Tan X, Zhong M, Xing J, Li W, Li D and Cao F: The role of catechins in regulating diabetes: An update review. *Nutrients* 14: 4681, 2022.
43. Russo B, Picconi F, Malandrucchio I and Frontoni S: Flavonoids and insulin-resistance: From molecular evidences to clinical trials. *Int J Mol Sci* 20: 2061, 2019.
44. Al-Ishaq RK, Abotaleb M, Kubatka P, Kajo K and Büsselberg D: Flavonoids and their anti-diabetic effects: Cellular mechanisms and effects to improve blood sugar levels. *Biomolecules* 9: 430, 2019.
45. Gołąbek KD and Regulska-Ilow B: Dietary support in insulin resistance: An overview of current scientific reports. *Adv Clin Exp Med* 28: 1577-1585, 2019.
46. Carta G, Murru E, Banni S and Manca C: Palmitic acid: Physiological role, metabolism and nutritional implications. *Front Physiol* 8: 902, 2017.
47. Sánchez-Alegria K, Bastián-Eugenio CE, Vaca L and Arias C: Palmitic acid induces insulin resistance by a mechanism associated with energy metabolism and calcium entry in neuronal cells. *FASEB J* 35: e21712, 2021.
48. Brown G: Glucose transporters: Structure, function and consequences of deficiency. *J Inher Metab Dis* 23: 237-246, 2000.
49. D'Alessandris C, Lauro R, Presta I and Sesti G: C-reactive protein induces phosphorylation of insulin receptor substrate-1 on Ser307 and Ser 612 in L6 myocytes, thereby impairing the insulin signalling pathway that promotes glucose transport. *Diabetologia* 50: 840-849, 2007.
50. White MF: Insulin signaling in health and disease. *Science* 302: 1710-1711, 2003.
51. Koren-Gluzer M, Aviram M and Hayek T: Paraoxonase1 (PON1) reduces insulin resistance in mice fed a high-fat diet, and promotes GLUT4 overexpression in myocytes, via the IRS-1/Akt pathway. *Atherosclerosis* 229: 71-78, 2013.
52. Petersen MC, Vatner DF and Shulman GI: Regulation of hepatic glucose metabolism in health and disease. *Nat Rev Endocrinol* 13: 572-587, 2017.
53. Ren Z, Xie Z, Cao D, Gong M, Yang L, Zhou Z and Ou Y: C-Phycocyanin inhibits hepatic gluconeogenesis and increases glycogen synthesis via activating Akt and AMPK in insulin resistance hepatocytes. *Food Funct* 9: 2829-2839, 2018.
54. Hattig M, Tavares CDJ, Sharabi K, Rines AK and Puigserver P: Insulin regulation of gluconeogenesis. *Ann N Y Acad Sci* 1411: 21-35, 2018.
55. Murray B and Rosenbloom C: Fundamentals of glycogen metabolism for coaches and athletes. *Nutr Rev* 76: 243-259, 2018.
56. Sullivan MA and Forbes JM: Glucose and glycogen in the diabetic kidney: Heroes or villains? *EBioMedicine* 47: 590-597, 2019.
57. Kamiyama M, Naguro I and Ichijo H: In vivo gene manipulation reveals the impact of stress-responsive MAPK pathways on tumor progression. *Cancer Sci* 106: 785-796, 2015.
58. Yudhani RD, Sari Y, Nugrahaningsih DAA, Sholikhah EN, Rochmanti M, Purba AKR, Khotimah H, Nugrahenny D and Mustofa M: In vitro insulin resistance model: A recent update. *J Obes* 2023: 1964732, 2023.



Copyright © 2023 Cho and Shaw. This work is licensed under a Creative Commons Attribution-NonCommercial-NoDerivatives 4.0 International (CC BY-NC-ND 4.0) License.